TECHNICAL PAPER

AI-Based Estimation of Swelling Stress for Soils in South Africa

Frank I. Aneke[1] · Kennedy C. Onyelowe[2] · Ahmed M. Ebid[3]

Abstract

Soil swelling is one of the major causes of structural failure, due to excessive moisture saturation and desaturation moisture. In situ measurement of swelling stress is somewhat impossible and requires tedious routine site observation. The use of artificial intelligence to predict the swelling stress of in situ soil is highly recommended, because of the complex behavior of soil upon moisture absorption. Because of this challenge, this study is channeled towards the prediction of swelling stress using basic geotechnical properties to save the challenges of repeating geotechnical experimental tests. In this study, the swelling stress of soils collected from 15 locations in 5 sites across South Africa has been predicted by using the artificial neural network (ANN), genetic programming (GP), and evolutionary polynomial regression (EPR)-based intelligent techniques. Multiple data were collected through laboratory experiments on the predictors: gravimetric moisture content (GMC), plasticity index (I_p), dry density (γ_d), free swell index (FSI), degree of saturation (S), matric suction (Ψ_m) and the target, and swelling stress (P_{sm}). This predictive model was aimed at proposing models, which will help earthwork designers and constructors in South Africa overcome the rampant visit to the laboratory in search of soil data needed for geotechnical engineering designs. The soils showed their potential for swelling, which was eventually confirmed by the sensitivity analysis of the intelligent models. The performance indices of the models showed that ANN outclassed the other techniques with a performance accuracy of 93.6% at an error of 1.9%. Also, the sensitivity analysis showed that the plasticity index and matric suction were the most influential to the models. With the predicted models, future earthworks in South Africa can quickly forecast swelling stress prior to designs and construction more so in hydraulically bound environments.

Keywords Swelling stress · Matric suction · Expansive soil · Artificial intelligence · ANN · EPR · GP

✉ Frank I. Aneke
   AnekeF@ukzn.ac.za

Extended author information available on the last page of the article

1 Introduction

Expansive soil underlies over one-third of the world's land surface, and it is often found in arid and semi-arid regions. South Africa as a country is situated between arid and semi-arid regions; hence, this caused 50 to 65% of South African soil to be expansive (Diop et al. 2011). This implies that expansive soils are always in unsaturated conditions as they are situated above the groundwater table. On that note, damages caused by expansive soils to buildings, roads, pipelines, and other geotechnical structures upon contact with water are much higher than the damage caused by floods, hurricanes, tornadoes, and earthquakes combined (Jones and Holtz 1973). More so, expansive soil undergoes significant volumetric changes upon contact with water, hence causing severe swelling, shrinkage, and desiccation cracks which if not properly predicted and mitigated could cause colossal damage to infrastructures. Therefore, it is imperative to intelligently predict the swelling stress of an expansive soil because swelling stress governs the amount of soil volume change which is one of the designs in geotechnical engineering rather than a frequent visit to the laboratory that is somewhat tedious and time-consuming. However, in situ measurement of swelling stress is extremely challenging and somewhat impossible, especially in the existing geotechnical foundation system. It is also a fact that swelling stress negatively influences the settlement of the geotechnical system causing an impediment to the desired use of the foundation through the reduction of the design life of the structure (Punthutaecha et al. 2006; Aneke et al. 2018; Aneke et al. 2021a, b).

Often geotechnical engineers are faced with the most crucial challenges of analyzing the mechanics of fine-grained soil while identifying and evaluating its vulnerability to contraction and expansion problems. Because the rate of swelling and shrinkage in expansive soil depends on the number of clay minerals. For instance, clayey soils expand and contract at a significant degree whereas sand and gravel shrink slightly. Many published studies have suggested the correlation of compression index (C_c) and the basic soil properties utilizing advanced models (Benbouras et al. 2018; Samui et al 2019; Moayedi et al. 2020). However, only a few widely accepted empirical equations have been proposed in the literature to estimate the swelling index (C_s) from physical soil parameters, such as the natural water content, the plasticity index, the liquid limit, the specific gravity, and others. Therefore, the need to intelligently predict swelling stress utilizing soft computing and genetic programming has become imperative. Failure and the challenges of analyzing swelling mechanism will continue to cause disturbances to foundations which can result in service life impairment of roads, buildings, pipelines, and other lightly loaded structures (Aneke et al. 2015; Ermias et al. 2017; Chu et al. 2018; Aneke et al. 2021a, b). In this regard, several scholars have used numerical analysis, statistical models, mathematical models, coupled artificial intelligence, and soft computing models to predict swelling stress (Ly et al. 2019; Mawlood and Hummadi 2020; Amin Benbouras and Alexandru-Ionut 2021; Aneke and Nkwonta 2021; Guo et al. 2021).

Artificial intelligence techniques for predicting the swelling stress of expansive soil have demonstrated a substantial degree of success, as an alternative approach

to data processing and analysis in various areas of engineering (Singh et al. 2013; Sharma et al. 2017). These techniques are flexible and dynamic and have a wide range of tolerance for uncertainty which makes them more reliable in handling complex geotechnical problems.

Ikizler et al. (2010) used grain density, LL, PL, PI, SL (shrinkage limit), OMC (optimum moisture content), MDD (maximum dry density), and K (hydraulic conductivity) to construct an ANN model that estimates swelling pressures of clay-rich soils. At first, the lateral and vertical swelling pressures were measured with different thicknesses of expanded polystyrene (EPS) geofoam placed between one of the vertical walls of the steel testing box and the expansive soil. Then, artificial neural network was trained using these pressures for the prediction of transmitted lateral swelling pressure and vertical swelling pressures on a retaining structure. Results obtained from this study showed that neural network-based prediction models could satisfactorily be used in obtaining the swelling pressures of the expansive soils.

Yilmaz and Kaynar (2011) applied multiple regression, radial basis function, multilayer perceptron, and ANFIS methods for the prediction of the swell potential of soils. In their study, they presented the use of MLP and RBF functions of ANN (artificial neural networks) and ANFIS (adaptive neuro-fuzzy inference system) for the prediction of S% (swell percent) of soil which was described and compared with the traditional statistical model of MR (multiple regression). However, the accuracies of ANN and ANFIS models may be evaluated relatively similarly. It was found that the constructed RBF exhibited a high performance than MLP, ANFIS, and MR for predicting S%. The performance comparison showed that a soft computing system is a good tool for minimizing uncertainties in soil engineering projects.

Ikizler et al (2014) provided a new estimation model to predict the pressures developed using experimental data. The data were collected in the laboratory using a newly developed device and experimental setup also. In the experimental setup, a rigid steel box was designed to measure transmitted swelling pressures in lateral and vertical directions. In the estimation model, approaches of artificial neural networks (ANN) and adaptive neuro-fuzzy inference systems (ANFIS) are employed. In the first stage of the study, the lateral and vertical swelling pressures were measured with different thicknesses of expanded polystyrene geofoam placed between one of the vertical walls of the steel box and the expansive soil in the laboratory. Then, ANN and ANFIS approaches were trained using the results of the tests measured in the laboratory as input for the prediction of transmitted lateral and vertical swelling pressures. Results obtained showed that ANN-based prediction and ANFIS approaches could satisfactorily be used to estimate the transmitted lateral swelling pressure. Other than the prediction of swelling stress, the artificial intelligence approach can also be used to predict several other geotechnical properties. Tizpa et al. (2015) presented artificial neural network prediction models which relate compaction characteristics, permeability, and soil shear strength to soil index properties. A database including a total number of 580 data sets was compiled. The database contains the results of grain size distribution, Atterberg limits, compaction, permeability measured at different levels of compaction degree (90–100%), and consolidated–drained triaxial compression tests. Comparison between the results of the developed models and experimental data indicated that predictions are within

a confidence interval of 95%. According to the performed sensitivity analysis, the Atterberg limits and the soil fine content are the most important variables in predicting the maximum dry density and optimum moisture content. Another aspect that is coherent from the sensitivity analysis is the considerable importance of the compaction degree in the prediction of the permeability coefficient. However, it can be seen that the effective friction angle of shearing is highly dependent on the bulk density of the soil.

Since unsaturated soil is typically located at the vadose zone above the groundwater table, this study is geared towards developing empirical models that correlate suction, gravimetric moisture content (GMC), plasticity index, dry density, and free swell index and degree of saturation to predict the swelling stress of three South African expansive soils. Generally, the developed models rationally predicted reliable results for expansive soils when validated with independent data sets without going through tedious processes. The developed models are also trusted to save high costs accompanied by running oedometer tests and time-consuming.

2 Materials and Methods

2.1 Material Preparation

2.1.1 Soil

The soil samples used herein were sampled from 4 different sites across Free State (i.e., Bloemfontein, Welkom, Bethlehem, and Winburg). The investigated soil is of vertisol characteristics, and it formed the parent soil across this province with excessive expansiveness and compressibility. Thus, they portray significant volumetric change upon contact with water, and these soils are categorized as one of the problematic soils in South Africa (Diop et al. 2011, Aneke et al. 2021a, b). Three different samples were collected from each visit, and they are labeled alphabetically as soil A, B, and C. As such, Fig. 1 presents the 4 visited sites where the soil samples were collected as highlighted in a green circle. Different cores were drilled at each site, and representative soil samples were collected at a depth of 1.2 m and sealed in airtight plastic bags to minimize moisture loss for the subsequent soil testing.

The collected soil samples were classified according to ASTM D2487-17 standard practice for engineering purposes. Based on the test results, the soil sample classifications range from CH to CL, with predominant clay contents and high plasticity. The grain size analysis of the soil samples was achieved through blends of different particle sizes. The blending of the particle size was applied to minimize grain size discrepancies that might influence the test results. Firstly, dry sieving was conducted by passing soil grains through a 9.5-mm sieve size, followed by additional sieving through aperture sieve sizes of 4.75 mm and 75-µm sieves to separate fines, sand, and gravel. The hydrometer analysis was also conducted as 75 to 85% of fines passed through the 75-µm sieve as summarized in Table 1. The purpose of the hydrometer analysis is to further differentiate the percentages of silt and clay representative from the fines following ASTM D1140.
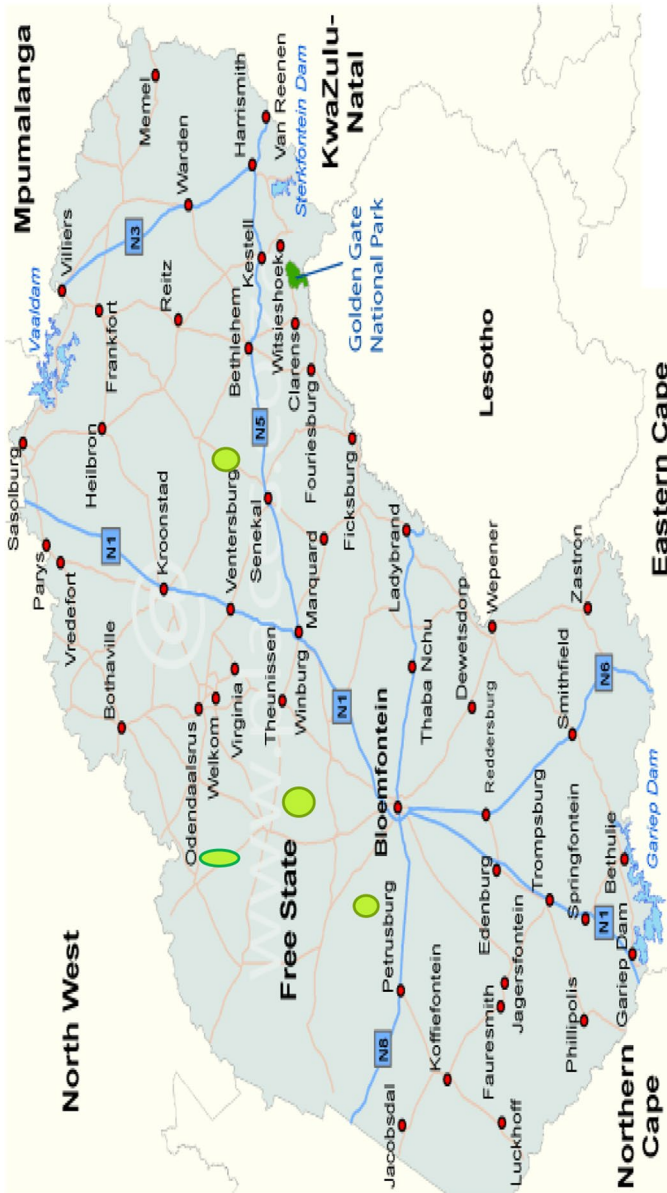
Fig. 1 The visited sites are highlighted in green color

Table 1 Summary of soil properties used in the study

Designation		LL (%)	I_p (%)	L_S (%)	Fines (%)		Gravel (%)	G_s	USCS
Sites	Soils				Silt	Sand			
BLM 1	Soil A	69.11	43.93	18.9	71.38	18.32	10.30	2.75	CH
	Soil B	65.23	38.11	22.13	62.45	21.24	16.31	2.78	CH
	Soil C	64.18	35.71	16.42	59.20	27.19	13.61	2.74	CH
WLK 2	Soil A	61.30	38.25	13.68	55.25	28.83	15.92	2.77	CH
	Soil B	74.32	50.11	15.48	68.11	18.18	13.71	2.73	CH
	Soil C	45.20	22.10	11.24	39.27	40.24	20.49	2.75	CL
BHM 3	Soil A	75.41	35.47	13.83	67.98	20.92	11.10	2.71	CH
	Soil B	71.25	29.54	12.93	64.78	21.98	13.24	2.76	CH
	Soil C	66.24	24.13	15.24	58.23	28.66	13.11	2.74	CH
WBG 4	Soil A	71.54	48.21	16.71	62.52	20.82	16.66	2.73	CH
	Soil B	42.61	19.32	8.11	35.21	42.15	22.64	2.69	CL
	Soil C	45.28	21.31	9.28	38.54	40.21	21.25	2.68	CL

G_s, specific gravity; *USCS*, universal soil classification system

Based on the consistency test as presented in Table 1, the liquid and shrinkage limit results imply that the investigated soils possess a degree of expansion. The plasticity values of the soils are within the range of 35 to 50%, whereas the obtained linear shrinkage is within the value range of 15 to 23%. In the winter season, when the samples were sampled, the soil generally experiences a net water deficit given the semi-arid climate prevalent in the province. The degree of saturation ranges from 82 to 95, and the value reflects the unsaturated condition of the soil in the field because the high liquid limit and plastic limit indicate high-water retention capability due to the double-layer structure of the clay minerals available in the soil. It is noted that the percentages of expansive clay minerals such as smectite, montmorillonite, kaolinite, and vermiculite also contributed to the soil–water retention capacity of the soils.

The index properties of clayey material depend on the type and content of clay minerals, which considerably influence the swelling stress of expansive soils (Changxi et al. 2019). Therefore, to evaluate the mineralogical compositions responsible for swelling activities, the investigated soils were subjected to X-ray diffraction (XRD) testing using the Rigaku TTRA III diffractometer, and tests were performed at Cu Kα radiation (1.5418 Å) level as presented in Table 2. The presented XRD result analysis also confirms that the investigated soils are expansive consisting of dominant phases of smectite, illite, silica, calcite, and other clay minerals evaluated at trace level.

2.1.2 Sample Preparations

Prior to sample preparation, Proctor compaction tests were conducted on the soil samples following ASTM D698-12(2021), to determine the optimum moisture content (OMC) with the corresponding maximum dry density (MDD) of the soil. Due

Table 2 Soil mineralogical compositions (X-ray diffraction result)

Sites	Soils	Smectite	Silica	K-feldspar	Plagioclase	Illite	Calcite
BLM 1	Soil A	71.74	13.41	9.91	1.85	1.89	1.22
	Soil B	67.05	19.98	10.66	2.31	< <	< <
	Soil C	71.74	13.40	9.91	1.85	1.89	1.22
WLK 2	Soil A	61.30	13.25	6.95	5.15	8.13	5.22
	Soil B	70.18	11.12	5.14	4.11	2.31	3.14
	Soil C	34.26	30.75	20.32	7.04	2.11	5.52
BHM 3	Soil A	64.23	14.36	8.93	5.98	4.58	2.10
	Soil B	67.47	15.54	8.49	4.15	3.21	1.14
	Soil C	65.50	10.45	7.03	6.37	6.14	4.51
WBG 4	Soil A	63.37	20.34	10.71	1.80	2.43	1.35
	Soil B	61.14	11.93	19.01	2.63	3.31	1.98
	Soil C	59.53	27.47	9.19	3.81	< <	< <

BLM, Bloemfontein; *WLK*, Welkom; *BHM*, Bethlehem; *WBG*, Winburg

to the high soil–water retention capacity, the investigated soils rendered moisture contents within the range of 18.24 to 33.31% from the dry to the wet side of the optimum. This implies that the soils constitute high plasticity with significant swelling potentials, whereas the dry densities at the optimum moisture content range from 17.74 to 21.85 kN/m^3 for the investigated soils. The soil samples were prepared at various dry densities with their corresponding moisture contents, as initially obtained from the compaction test. The soils were prepared for a series of tests mentioned earlier in this study, by weighing out given quantities of soil. The molding moisture contents that were determined from the Proctor compaction test were measured out followed by thorough mixing of the measured soil and water contents. The mixing continued until a homogeneous soil mixture was obtained. The soil mixtures were covered in airtight plastic bags for 8 h before specimen fabrication for the series of geotechnical testing mentioned earlier in this study to ensure uniform distribution of moisture. The preliminary compaction test was used as a guide to determine the required quantities of water for the specimen's fabrication; thus, the specimens were deemed suitable for testing when the density after preparation was at least 97% of the targeted MDD after specimen fabrication.

2.2 Experimental Methods and Data Collection

2.2.1 Laboratory Work

The present study is focused on the prediction of swelling stress by applying artificial intelligence soft computing programming as well as using laboratory-generated data for the training of artificial intelligent programs. The free swell index was conducted following the Indian standard IS-2720 (Part 40, 2002) test method. The main objective of this test is to evaluate the swelling potential of expansive soils.

The soil used for this test was passed through a 425-µm sieve size (#40); this sieve size was selected because it represents 90% of the fines from the soil. The soils were oven-dried at a temperature of 115 °C, and 2 graduated cylinders were filled with water and kerosene to the level of 100 ml. Subsequently, 10 g of the representative soil samples was placed into each cylindrical jar followed by vigorous shaking and agitation for 15 min. The graduated cylindrical jar after shaking was placed on a flat surface and allowed to settle. The initial volume of the soil placed into the jars was recorded followed by the last reading after 48 h of taking the initial readings. The soil placed in the jar containing kerosene did change in volume as it was used as the control, whereas the volume of the soil in the jar containing water recorded a significant increase in volume. Therefore, the free swell index is the expression in Eq. 1.

$$FSI = \left[(V_s - V_k)/V_k \right] \times 100\% \tag{1}$$

where FSI is the free swell index, V_k is the volume of soil in kerosene, and V_s is the volume of soil in water.

The filter paper test was used in this study to determine the soil matric suction since the soil is unsaturated. However, the filter paper test was conducted following ASTM 5298 (2016). Prior to the specimen fabrication for the filter paper test, the samples were prepared with different moisture contents; then, the specimens were shaped to have a dimension of 85 mm and 70 mm of diameter and height. Subsequently, specimens were cut in half, and three filter papers were sandwiched between the sliced soils. After the filter papers were sandwiched, the joint was sealed off with electric tape to eliminate moisture loss for the filter paper. The taped specimens with sandwiched filter papers were placed in different jars and a poly-vinyl chloride (PVC) ring of 40 mm diameter and 5 mm thickness was placed on top of each taped specimen and non-contact filter papers were subsequently placed on top of the poly-vinyl chloride (PVC) ring. The prepared specimens were labeled and placed in an ice chase box capable of maintaining 240 °C temperature for 14 days. After 14 days, the contact and no-contact filter papers were retrieved and weighed, and their water contents were determined following the procedures suggested by Bulut and Leong (2008). Then, filter paper moisture contents were converted to total suction and matric suction using Eqs. 2 and 3.

$$Log(kPa) = -0.0769\omega_f + 5.2266, \tag{2}$$

$$Log(kPa) = -0.0126\omega_f + 2.3361 \tag{3}$$

where ω is the filter paper water content.

Zero Swelling Test The zero swelling test is a measure of soil swelling counter loading with contact with water up until no further swelling is recorded. In this study, the ZST was conducted following IS 2720 (Part 41, 1977). The soil samples passing through an ASTM sieve size of 4.75 mm (#4) were used due to the high content of fines. The specimens were prepared at various moisture contents and corresponding dry unit weights, according to the initial compaction test. After

compaction, the specimens were demolding and shaped to bear 25 mm in height and 75 mm in diameter size to fit into the oedometer ring. It was then wetted on a high-pressure oedometer frame under vertical stress of 0.1 MPa using distilled water as the specimens are loaded. Once the swelling starts, the vertical load was increased to prevent further vertical swelling. During this process, maximum swell and vertical strain were allowed as presented in Fig. 2. The swelling was deemed complete when no further swelling was recorded by the swelling dial gauge. The total applied load was summed as Eq. 4 which is used to calculate the swelling stress at each molding moisture content. The zero swelling experimental setups are shown in Fig. 2.

$$P_s(\text{kPa}) = \left(\sum_{i}^{n} = 1 M_i \times g \times b_r / \pi(\varnothing^2)/4 \right)/100 \qquad (4)$$

where P_s is the swelling stress in kPa, $\sum_{i}^{n} = 1 M_i$ is the total sum of surcharge, g is the acceleration due to gravity 9.81 m/s^2, b_r is the beam ratio of the oedometer arm, and $\pi(\varnothing^2)/4$ is the internal area of the ring.

2.2.2 Collected Database and Statistical Analysis

The physical and mechanical proprieties of 60 soil samples were tested following these soil parameters gravimetric moisture content (GMC) (%), plasticity index (I_p) (%), dry density (γ_d) (t/m^3), free swell index (FSI) (%), degree of saturation (S) (%), matric suction (Ψ_m) (MPa), and swelling stress (P_{sm}) (MPa). The measured records were divided into two sets, i.e., training and validation. Thus, 40 records were used for the training exercise whereas 20 records were used for validation purposes as presented in Table 3 with the inclusion of the complete data set. Furthermore, Tables 4 and 5 summarize the statistical characteristics and the Pearson correlation matrix of the data set as the histograms for both inputs and outputs are demonstrated in Fig. 3. The histogram results revealed that FSI recorded the highest frequency value, followed by dry unit weight, GMC, and matric suction. It is also evident that the plasticity index and degree of saturation recorded the same frequency value (Table 6). The frequency provokes an increment in the quantity of data; therefore, it enhances the performance which adjusts the magnitude of change in each variable value and most likely influences the predictability of the model.

2.3 Research Program

Besides the traditional multi-linear regression (MLR) technique, three different artificial intelligent (AI) techniques were used to predict the shrinkage limit of the tested soil samples. These techniques are genetic programming (GP), artificial neural networks (ANN), and polynomial linear regression optimized using a genetic algorithm which is known as evolutionary polynomial regression (EPR). All three developed models were used to predict the values of swilling stress (P_{sm}) using the measured gravimetric

Fig. 2 Zero swelling test setup

Table 3 The used database

GMC (%)	I_p (%)	γ_d (t/m³)	FSI (%)	Ψ_m (MPa)	S (%)	P_{sm} (MPa)
Training set						
0.09	0.50	1.25	0.20	6.941	0.85	0.73
0.12	0.42	1.66	0.18	5.076	0.85	0.68
0.15	0.37	1.73	0.16	3.789	0.85	0.60
0.23	0.28	1.59	0.12	2.593	0.85	0.53
0.28	0.10	1.29	0.02	0.921	0.85	0.40
0.10	0.40	1.25	0.18	8.517	0.94	0.70
0.13	0.39	1.56	0.16	6.843	0.94	0.68
0.18	0.28	1.69	0.13	4.989	0.94	0.58
0.23	0.20	1.42	0.10	3.295	0.94	0.52
0.28	0.10	1.21	0.01	1.613	0.94	0.42
0.09	0.40	1.15	0.20	6.498	0.85	0.70
0.13	0.38	1.76	0.18	5.145	0.85	0.65
0.18	0.30	1.66	0.15	4.250	0.85	0.60
0.23	0.20	1.69	0.04	2.898	0.85	0.51
0.27	0.10	1.35	0.02	1.040	0.85	0.40
0.08	0.45	1.61	0.18	6.541	0.92	0.72
0.13	0.39	1.89	0.15	5.976	0.92	0.66
0.16	0.31	1.94	0.10	4.689	0.92	0.61
0.25	0.28	1.75	0.08	2.793	0.92	0.51
0.28	0.10	1.62	0.04	1.121	0.92	0.45
0.09	0.50	1.55	0.18	8.628	0.97	0.73
0.12	0.40	1.75	0.16	6.754	0.97	0.65
0.18	0.38	1.85	0.10	5.898	0.97	0.55
0.25	0.36	1.89	0.08	2.895	0.97	0.51
0.30	0.12	1.56	0.06	1.413	0.97	0.41
0.10	0.35	1.42	0.18	6.398	0.83	0.68
0.14	0.30	1.59	0.16	5.345	0.83	0.60
0.21	0.26	1.68	0.13	3.450	0.83	0.55
0.26	0.18	1.60	0.08	1.998	0.83	0.48
0.33	0.10	1.30	0.04	1.240	0.83	0.42
0.09	0.36	1.65	0.2	8.534	0.95	0.73
0.13	0.30	1.95	0.17	6.098	0.95	0.62
0.19	0.29	2.18	0.15	4.643	0.95	0.60
0.24	0.23	2.01	0.11	2.134	0.95	0.51
0.29	0.11	1.62	0.07	1.378	0.95	0.46
0.10	0.36	1.55	0.20	5.278	0.97	0.65
0.14	0.30	1.92	0.18	4.465	0.97	0.58
0.19	0.25	2.09	0.15	3.087	0.97	0.58
0.27	0.21	1.90	0.12	2.598	0.97	0.47
0.30	0.10	1.60	0.10	1.091	0.97	0.41

Table 3 (continued)

GMC (%)	I_p (%)	γ_d (t/m³)	FSI (%)	Ψ_m (MPa)	S (%)	P_{sm} (MPa)
Validation set						
0.10	0.38	1.81	0.20	6.395	0.95	0.66
0.14	0.32	2.16	0.15	4.525	0.95	0.65
0.19	0.28	2.28	0.12	3.272	0.95	0.58
0.24	0.19	2.17	0.08	2.010	0.95	0.52
0.30	0.10	1.88	0.06	1.481	0.95	0.40
0.10	0.43	1.65	0.16	7.071	0.92	0.70
0.14	0.39	1.88	0.14	5.884	0.92	0.67
0.19	0.34	2.06	0.12	3.959	0.92	0.56
0.24	0.25	1.80	0.10	2.183	0.92	0.48
0.30	0.12	1.60	0.03	1.128	0.92	0.43
0.10	0.35	1.77	0.18	4.263	0.82	0.68
0.14	0.17	2.00	0.16	3.989	0.82	0.63
0.19	0.15	2.24	0.13	2.914	0.82	0.56
0.23	0.14	2.10	0.10	2.029	0.82	0.50
0.243	0.10	1.98	0.04	0.667	0.82	0.46
0.09	0.21	1.97	0.20	4.331	0.85	0.70
0.12	0.18	2.11	0.16	3.708	0.85	0.65
0.17	0.14	2.26	0.12	2.707	0.85	0.57
0.24	0.12	2.24	0.08	1.715	0.85	0.50
0.28	0.08	2.12	0.02	0.763	0.85	0.42

Table 4 Statistical analysis of the collected database

	GMC (%)	I_p (%)	γ_d (t/m³)	FSI (%)	Ψ_m (MPa)	S (%)	P_{sm} (MPa)
Training set							
Min	0.08	0.22	1.15	0.60	0.92	0.83	0.35
Max	0.33	0.50	2.18	1.50	8.63	0.97	0.87
Avg	0.19	0.37	1.64	1.04	4.22	0.91	0.59
SD	0.08	0.08	0.24	0.28	2.25	0.05	0.14
Var	0.40	0.22	0.15	0.27	0.53	0.06	0.24
Validation set							
Min	0.09	0.19	1.60	0.60	0.67	0.82	0.35
Max	0.30	0.48	2.28	1.40	7.07	0.95	0.87
Avg	0.19	0.28	2.00	0.88	3.25	0.89	0.58
SD	0.07	0.12	0.20	0.31	1.79	0.05	0.13
Var	0.37	0.41	0.10	0.36	0.55	0.06	0.23

moisture content (GMC) (%), plasticity index (I_p) (%), dry density (γ_d) (t/m³), free swell index (FSI) (%), degree of saturation (S) (%), and matric suction (Ψ_m) (MPa). Each model of the three developed models was based on a different approach (evolutionary

Table 5 Pearson correlation matrix

	GMC	I_p	γ_d	FSI	Ψ_m	S	P_{sm}
GMC	1.00						
I_p	0.01	1.00					
γ_d	-0.06	-0.38	1.00				
FSI	0.03	0.29	-0.28	1.00			
Ψ_m	-0.89	0.27	-0.19	0.09	1.00		
S	0.02	0.45	0.06	0.28	0.20	1.00	
P_{sm}	-0.94	-0.03	-0.09	-0.03	0.84	-0.14	1.00
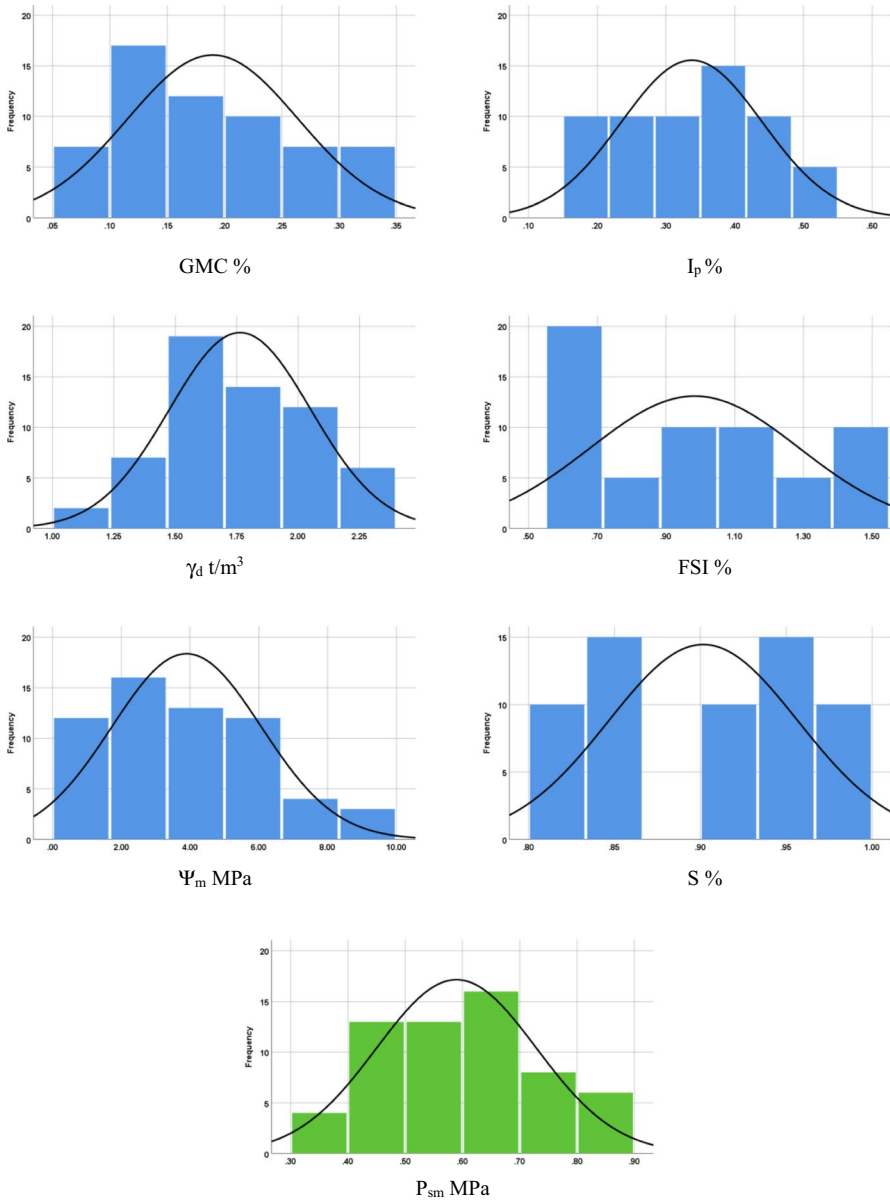
Fig. 3 Distribution histograms for inputs (in blue) and outputs (in green)

approach for GP, mimicking biological neurons for ANN, and optimized mathematical regression technique for EPR). However, for all developed models, prediction accuracy was evaluated in terms of the sum of squared errors (SSE).

Table 6 Connection weights for the developed ANN

		Hidden layer 1				Output layer
		H (1:1)	H (1:2)	H (1:3)	H (1:4)	P_{sm}
Input layer	Bias	−0.71	0.03	−0.37	−0.61	
	GMC	−0.10	−0.84	−0.81	0.32	
	I_p	−0.07	−0.52	−0.70	−1.32	
	γ_d	−0.21	0.38	0.22	0.65	
	FSI	0.53	−0.27	0.34	0.38	
	Ψ_m	0.12	−0.01	−0.08	0.65	
	S	−0.29	0.39	0.27	0.50	
Hidden layer 1	Bias					−0.01
	H (1:1)					0.85
	H (1:2)					0.84
	H (1:3)					0.72
	H (1:4)					−0.95

The following section discusses the results of each model. The accuracies of developed models were evaluated by comparing the (SSE) between predicted and calculated swilling stress (P_{sm}) values. The results of all developed models are summarized in Table 7.

3 Results and Discussions

3.1 Preliminary Results

Geotechnical sensitivity analysis was conducted prior to artificial intelligence prediction of the swelling stress to evaluate which of the geotechnical index properties is highly sensitive to swelling stress. Figure 4 presents the geotechnical sensitivity analysis of the individual geotechnical properties like plasticity index, free swell index, gravimetric moisture content (GMC), and matric suction. Based on the obtained results, it was noted that the GMC has the highest sensitivity to swelling stress prediction compared to the rest of the geotechnical properties. In the order of hierarchy, the gravimetric moisture content is the highest

Table 7 Performance accuracies of developed models

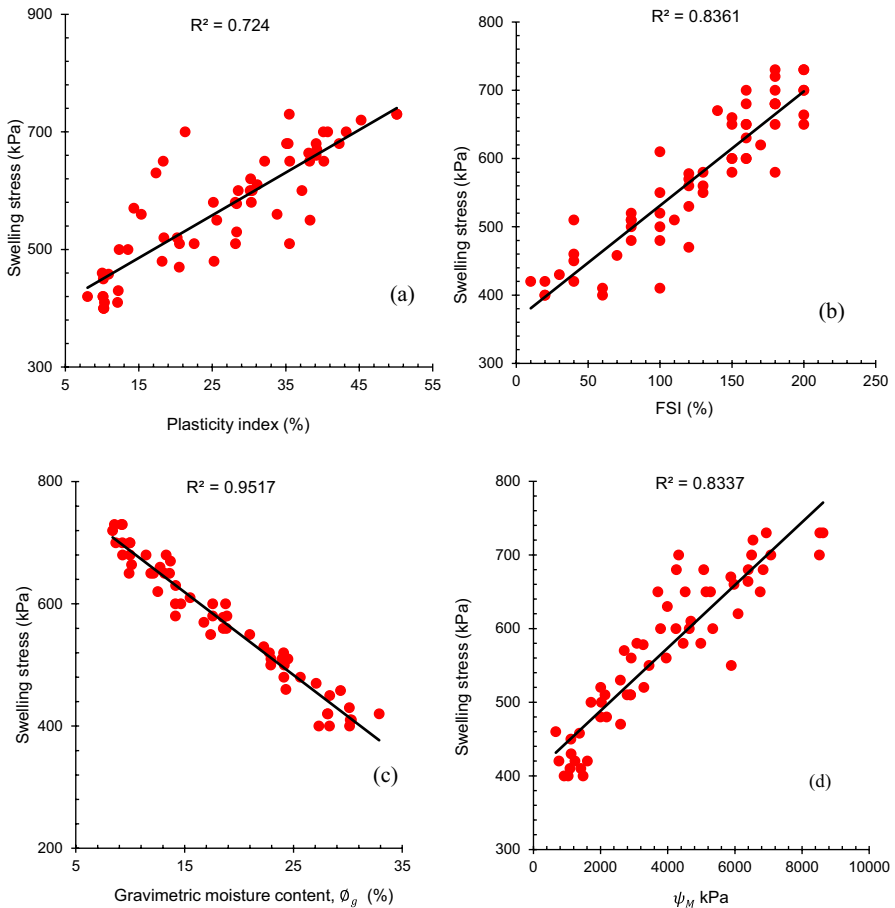| Technique	Developed equation	Error %	R^2
MLR	Equation (1)	2.4	0.907
GP	Equation (2)	2.4	0.907
ANN	Equation (3)	1.9	0.936
EPR	Equation (3)	2.1	0.930

Fig. 4 Correlation relationship behavior for **a** swelling stress and plasticity index, **b** swelling stress and FSI, **c** swelling stress–matric suction, and **d** swelling stress and suction

sensitive property index, followed by the free swell index, matric suction, and plasticity index, respectively. The high sensitivity of GMC on swelling stress was a result of the high smectite mineral contained, diffused double-layer structure, and absorption capacity of the investigated soils. Hence, the increased soil plasticity was expected due to the high liquid limit value of the soil because water is needed to make the mixture more plastic thereby resulting in a higher coefficient of determination (R^2) of 95% compared to FSI, matric suction, and plasticity that render lower R^2 of 84%, 83%, and 73%, respectively. Furthermore, the dry unit weight and degree of saturation are a function of GMC. Therefore, the degree of saturation and dry unit weight responds differently as the GMC increases. Notably in this study, it could be concluded that the GMC significantly influences the response of the soil swelling stress, though the obtained results agree with the study published by Abbey et al. (2017), Abbey et al. (2020), and Aneke

and Nkwonta (2021), which stated that the several additional soil properties like liquid limit, plastic limit, plasticity index, or unit weight influence the swelling stress; thus, moisture content is the principle index property that controls the other mechanical soil properties. They also concluded that water content has statistical significance in the estimation of swell pressure for the expansive soil. Figure 5 presents the microstructural surface configuration of the 15 soil samples
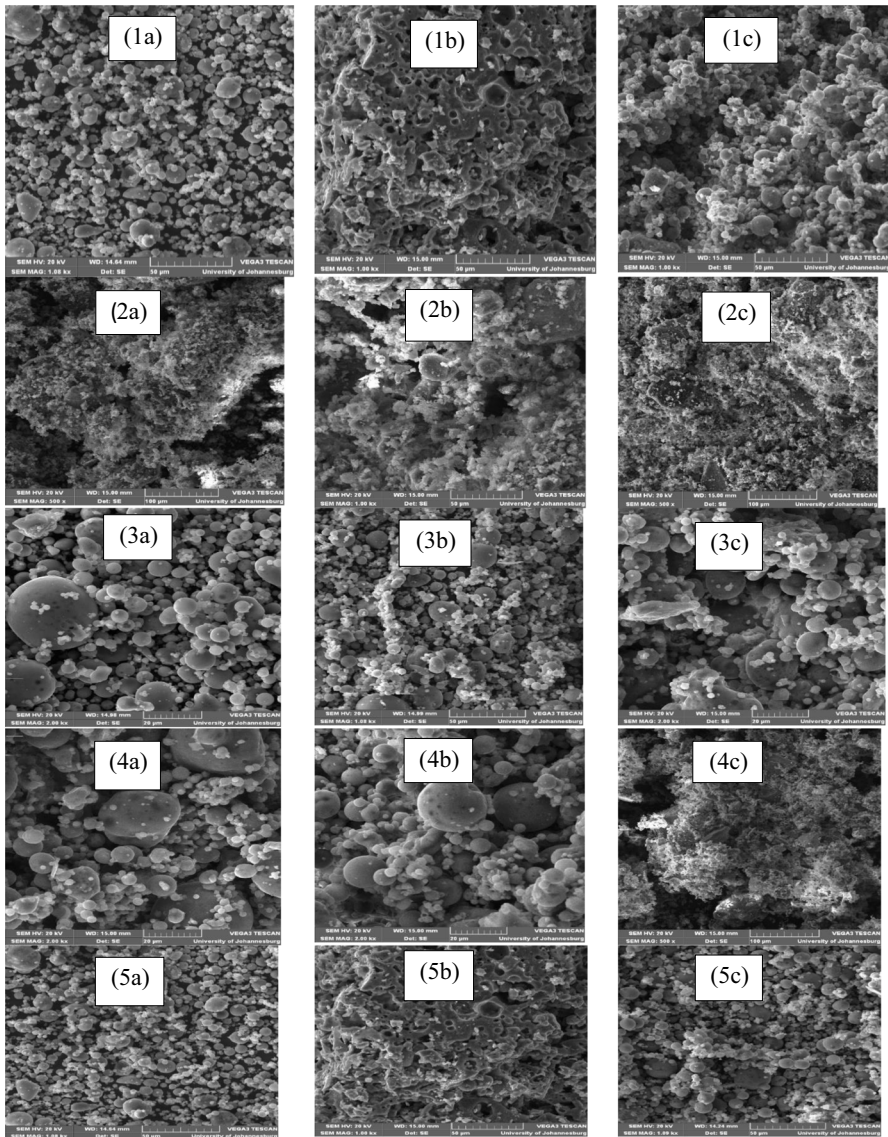

Fig. 5 SEM of site 1: soils a, b, and c; site 2: soils a, b, and c; site 3: soils a, b, and c; site 4: soils, a, b, and c; and site 5: soils a, b, and c

collected from the 5 locations across South Africa. It can be seen that soils from sites 1 and 5 are more consistent in surface behavior compared to the other three. These behaviors help to study the surface response to suction and the resultant swelling stress upon exposure to moisture ingress and impregnation.

3.2 Prediction of Swilling Stress (P_{sm})

3.2.1 Model (1)—Using (MLR) Technique

Prior to the intelligent prediction of the swelling pressure, a geotechnical sensitivity analysis was first conducted to identify the most sensitive soil index properties with the highest influence on the swelling stress. It is noted that swelling stress is exponentially relative to dry unit weight; hence, it is dependent on the initial GMC of the soil. Furthermore, the swelling stress is less affected upon soil saturation, rather it increases with the initial dry unit weight of the soil but decreases as the initial GMC shift from the dry side to the wet side of the optimum. This trend behavior agrees with the predictions of conceptual models that consider the interaction between the responses of the microstructure and the macrostructure as published elsewhere by Aneke et al. (2022) and Ikechukwu and Mostafa (2022) which indicates that moisture content in the soil material mobilizes the secondary effect on matric suction.

Therefore, the trend influence of the GMC on swelling stress mobilized this study to further investigate the results obtained from the preliminary geotechnical sensitivity analysis. Therefore, the traditional multi-linear regression (MLR) technique was used as a benchmark to evaluate the accuracies of the three (AI) techniques. The developed MLR was generated using the MS-EXCEL Add-in regression module. The output expression for P_{sm} is presented in Eq. 5 while Fig. 3 shows its fitting curve accuracy. The average error % of this model is 2.4% with a coefficient of determination (R^2) value of 0.907.

$$P_{sm} = 1.31 - 1.9\text{GMC} - 0.261I_p - 0.08\gamma_d - 0.004\text{FSI} - 0.005\psi_m - 0.2S \quad (5)$$

From the presented expression in Eq. 5, more geotechnical index properties, i.e., degree of saturation and dry unit weight, were considered to intelligently evaluate the most influential among the considered properties. It was noted that the listed mechanical soil properties were negatively correlated to the swelling stress; this was expected because the above-mentioned soil properties negatively influence the swelling pressure.

3.2.2 Model (2)—Using (GP) Technique

The developed GP model started with one level of complexity and settled at three levels of complexity. The population size, survivor size, and number of generations were 50,000, 15,000, and 75, respectively. Equation 6 presents the output formulas for P_{sm}, while Fig. 7b shows its fitness. The average error % of this equation is 2.4%, while the R^2 value is 0907.

$$P_{sm} = \frac{\mathrm{Ln(GMC.S)}}{(1.1S)^{7\mathrm{GMC}-1} - 3.15} \quad (6)$$

3.2.3 Model (3)—Using (ANN) Technique

A back-propagation ANN with one hidden layer and (Hyper Tan) activation function was used to predict the same swilling stress (P_{sm}) values. The used network layout and its connotation weights are illustrated in Fig. 6 and Table 6. The average error % of this model is 1.9%, and the corresponding R^2 value is 0.936. The relation between calculated and predicted values is shown in Fig. 7c.

3.2.4 Model (3)—Using (EPR) Technique

Finally, the developed EPR model was limited to a hexagonal level; for 6 inputs, there are 924 possible terms ($462 + 252 + 126 + 56 + 21 + 6 + 1 = 924$) as follows:
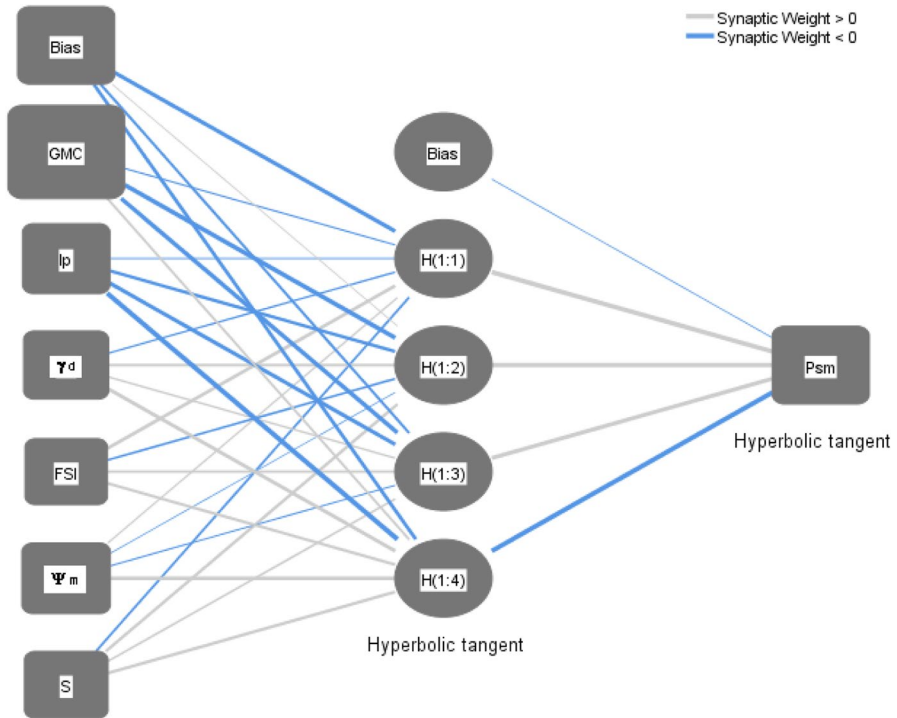
Fig. 6 Layout for the developed ANN and its connection weights
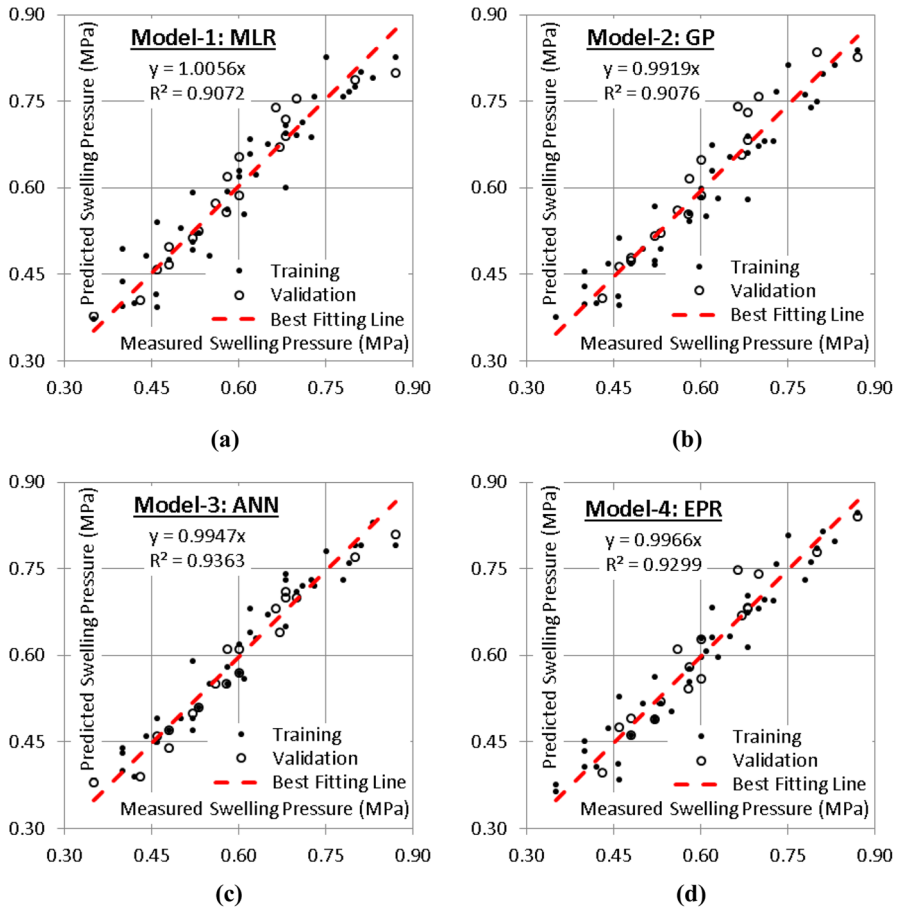
Fig. 7 Relation between predicted and calculated P_{sm} values using the developed models

$$\sum_{i=1}^{i=6}\sum_{j=1}^{j=6}\sum_{k=1}^{k=6}\sum_{l=1}^{l=6}\sum_{m=1}^{m=6}\sum_{n=1}^{n=6}X_i.X_j.X_k.X_l.X_m.X_n + \sum_{i=1}^{i=6}\sum_{j=1}^{j=6}\sum_{k=1}^{k=4}\sum_{l=1}^{l=6}\sum_{m=1}^{m=6}X_i.X_j.X_k.X_l.X_m$$

$$+\sum_{i=1}^{i=6}\sum_{j=1}^{j=6}\sum_{k=1}^{k=6}\sum_{l=1}^{l=6}X_i.X_j.X_k.X_l + \sum_{i=1}^{i=6}\sum_{j=1}^{j=6}\sum_{k=1}^{k=6}X_i.X_j.X_k + \sum_{i=1}^{i=6}\sum_{j=1}^{j=6}X_i.X_j + \sum_{i=1}^{i=6}X_i + C$$

GA technique was applied on these 924 terms to select the most effective 9 terms to predict the values of the swilling stress (P_{sm}) values. The output is illustrated in Eq. 7 and its fitness is shown in Fig. 7d. The average error % and R^2 values were 2.1% and 0.930 for the total data sets, respectively.

$$P_{sm} = 1.88 - 1.31\text{GMC} + \frac{Ip - 16\text{GMC}}{55\text{gd}.S.\text{GMC}.Ip} + \frac{\text{gd}.S}{3}(\text{gd} - 3.6Ip) - \frac{4.1\text{gd}.Ip.S + S - 0.5Ip}{11.3Ip^2}$$

$$(7)$$

4 Conclusions

This research presents three models using three (AI) techniques (GP, ANN, and EPR) to predict the swilling stress (P_{sm}) using the measured gravimetric moisture content (GMC) (%), plasticity index (I_p) (%), dry density (γ_d) (t/m^3), free swell index (FSI) (%), degree of saturation (S) (%), and matric suction (Ψ_m) (MPa). The traditional multi-linear regression (MLR) technique was used as a benchmark to evaluate the accuracies of the three (AI) techniques. The results of comparing the accuracies of the developed models could be concluded in the following points:

– The prediction accuracies of the three (AI) techniques are more than or equal to the accuracy of the traditional MLR technique.
– The prediction accuracies of MLR and GP models are the same (97.1% and 97.1%) while the accuracies of ANN and EPR are close (93.6% and 93%) which gives an advantage to the EPR model because its output is expressed in a simple equation and could be applied either manually or implemented in software unlike the complicated output of the ANN which cannot be applied manually.
– Weights of the ANN model and the formula of the (GP) model showed that P_{sm} value depends mainly on GMC values, and other parameters are secondary and have almost equal weights.
– GA technique successfully reduced the 924 terms of conventional PLR hexagonal formula to only 9 terms without significant impact on its accuracy.
– Like any other regression technique, the generated formulas are valid within the considered range of parameter values; beyond this range, the prediction accuracy should be verified.

Data Availability Data will be made available upon reasonable request.

Declarations

Ethical Approval This chapter does not contain any studies with human participants or animals performed by any of the authors.

Informed Consent Not applicable.

Conflict of Interest The authors declare no competing interests.

Open Access This article is licensed under a Creative Commons Attribution 4.0 International License, which permits use, sharing, adaptation, distribution and reproduction in any medium or format, as long as you give appropriate credit to the original author(s) and the source, provide a link to the Creative Commons licence, and indicate if changes were made. The images or other third party material in this article are included in the article's Creative Commons licence, unless indicated otherwise in a credit line to the material. If material is not included in the article's Creative Commons licence and your intended use is not permitted by statutory regulation or exceeds the permitted use, you will need to obtain permission directly from the copyright holder. To view a copy of this licence, visit http://creativecommons.org/licenses/by/4.0/.

References

Abbey, S.J., Ngambi, S., Ganjian, E.: Development of strength models for prediction of unconfined compressive strength of cement/byproduct material improved soils. Geotech. Test. J. **40**(6), 928–935 (2017)

Abbey, S.J., Eyo, E.U., Ngambi, S.: Swell and microstructural characteristics of high-plasticity clay blended with cement. Bull. Eng. Geol. Environ. **79**, 2119–2130 (2020). https://doi.org/10.1007/s10064-019-01621-z

Amin Benbouras, M., Alexandru-Ionut, P.: Prediction of swelling index using advanced machine learning techniques for cohesive soils. Appl. Sci. **11**(2), 536 (2021). https://doi.org/10.3390/app11020536

Aneke, F. I., Okonta, F. N., and Ntuli, F:. "Geotechnical properties of marginal highway backfill stabilized with activated fly ash" PhD Thesis, Dep. Of Civil Eng. Sci. And Built Envir. The University of Johannesburg, Gauteng, South Africa (2015)

Aneke, F. I., Mostafa, M. H., Moubarak, A.: Behaviour of unsaturated soils for road pavement structure under cyclic loading. PhD Thesis, Free State, South Africa: Department of Civil Engineering and Information Technology Central University of Technology (2018)

Aneke, F.I., Nkwonta, O.: Validation of semi-empirical models for the prediction of swelling stress for compacted unsaturated expansive soils. Civ. Eng. Archit. **9**(5), 1640–1658 (2021). https://doi.org/10.13189/cea.2021.090533

Aneke, F.I., Mohamed, M.H., Moubarak, A.: Resilient modulus and microstructure of unsaturated expansive subgrade stabilized with activated fly ash. Int. J. Geotech. Eng. **15**(8), 915–938 (2021a). https://doi.org/10.1080/19386362.2019.1656919

Aneke, F.I., Mohamed, M.H., Azza, M.: Swelling stress effects on shear strength resistance of subgrades. Int. J. Geotech. Eng. **15**(8), 939–949 (2021b). https://doi.org/10.1080/19386362.2019.1656445

Aneke, F.I., Onyelowe, K.C., Ebid, A.M., Light, I.N., Joy, T.A.: Predictive models of swelling stress—a comparative study between BP- and GRG-ANN. Arab. J. Geosci. **15**, 1438 (2022). https://doi.org/10.1007/s12517-022-10706-1

ASTM D698–12(2021). Standard test methods for laboratory compaction characteristics of soil using standard effort (12,400 ft-lbf/ft (600 kN-m/m)), ASTM International, West Conshohocken, PA, 2021, www.astm.org

ASTM D5298 (2008). Standard test method for measurement of soil potential (suction) using filter paper, D 5298; 04. 08, American Society for Testing and Materials, PA, USA, 2016. https://doi.org/10.1520/d5298-16

Benbouras, M. A., Kettab, R., Zedira, H., Petrisor, A., Mezouer, N., Debiche, F.: A new approach to predict the compression index using artificial intelligence methods. Mar. Georesour. Geotechnol. **6**, 704–720. (2018) [CrossRef]

Bulut, R., Leong, E.C.: Indirect measurement of suction. In: Tarantino, A., Romero, E., Cui, Y.J. (eds.) Laboratory and Field Testing of Unsaturated Soils. Springer, Dordrecht (2008). https://doi.org/10.1007/978-1-4020-8819-3_3

Changxi, H., Wang, X., Zhou, H., Liang, Y.: Factors affecting the swelling-compression characteristics of clays in Yichang, China. Adv. Civ Eng, **2019**, 6568208 (2019). https://doi.org/10.1155/2019/6568208

Chu, Y., Songyu, L., Bate, B., Lei, X.: Evaluation on expansive performance of the expansive soil using electrical responses. J. App. Geophys. **148**, 265–271 (2018). https://doi.org/10.1016/j.jappgeo.2017.12.001

Diop, S., Stapelberg, F., Tegegn, K., Ngubelanga, S., Heath, L.: A review of problem soils in South Africa. Counc. for Geosci. Rept. Num. 0062 (2011)

Ermias, B., Raghuvanshi, T.K., Abebe, B.: Landslide Hazard Zonation (LHZ) around Alemketema Town, North Showa Zone, Central Ethiopia—a GIS based expert evaluation approach. Int. J. Earth Sci. Eng. **10**(01), 33–44 (2017)

Guo, Q., Li, B., Chen, Y.: Intelligent model for the compressibility prediction of cement-stabilized dredged soil based on random forest regression algorithm. KSCE J. Civ. Eng. (2021). https://doi.org/10.1007/s12205-021-2202-3

Ikechukwu, A.F., Mostafa, M.M.H.: Swelling pressure prediction of compacted unsaturated expansive soils. JERA (2022). https://doi.org/10.4028/p-eq1419

Ikizler, S.B., Aytekin, M., Vekli, M., Kocabas, F.: Prediction of swelling pressures of expansive soils using artificial neural networks. Adv. Eng. Softw. **41**(4), 647–655 (2010)

Ikizler, S.B., Vekli, M., Dogan, E.: Prediction of swelling pressures of expansive soils using soft computing methods. Neural. Comput. Applic. **24**, 473–485 (2014). https://doi.org/10.1007/s00521-012-1254-1

I.S 2720, Part. 1., "Method of test for soils part 41 determination of soil swelling stress," Bureau of Indian Standards 2720. Part 40. 1977. https://law.resource.org/pub/in/bis/S03/is.2720.1.1983.pdf

Jones, D.E., Holtz, W.G.: Expansive soils-the hidden disaster. Civil Eng. ASCE **43**(8), 49–51 (1973)

Ly, H.-B., Le, T.-T., Le, L.M., Tran, V.Q., Le, V.M., Vu, H.-L.T., Nguyen, Q.H., Pham, B.T.: Development of hybrid machine learning models for predicting the critical buckling load of I-shaped cellular beams. Appl. Sci. **9**(24), 5458 (2019). https://doi.org/10.3390/app9245458

Mawlood, Y.I., Hummadi, R.A.: Large-scale model swelling potential of expansive soils in comparison with oedometer swelling methods. Iran. J. Sci. Technol. Trans. Civ. Eng. **44**, 1283–1293 (2020) [CrossRef]

Moayedi, H., Tien, B.D., Dounis, A., Ngo, P.T.T.: A novel application of league championship optimization (LCA): hybridizing fuzzy logic for soil compression coefficient analysis. Appl. Sci. **10**, 67 (2020)

Punthutaecha, K., Puppala, A.J., Vanapalli, S.K., Inyang, H.: Volume change behaviours of expansive soils stabilized with recycled ashes and fibres. J. Mater. Civ. Eng. **2006**(18), 295–306 (2006)

Samui, P., Hoang, N. D., Nhu, V. H., Nguyen, M. L., Ngo, P. T. T., Bui, D. T.: A new approach of hybrid bee colony optimized neural computing to estimate the soil compression coefficient for a housing construction project. Appl. Sci. **9**, 4912 (2019) [CrossRef]

Sharma, L.K., Vishal, V., Singh, T.N.: Developing novel models using neural networks and fuzzy systems for the prediction of the strength of rocks from key geomechanical properties. Measurement **102**, 158–169 (2017)

Singh, R., Vishal, V., Singh, T.N., Ranjith, P.G.: A comparative study of generalized regression neural network approach and adaptive neuro-fuzzy inference systems for prediction of unconfined compressive strength of rocks. Neural. Comput. Appl. **23**(2), 499–506 (2013)

Tizpa, P., Chenari, R.J., Fard, M.K., Machado, S.L.: ANN prediction of some geotechnical properties of soil from their index parameters. Ara. J. Geosci. **8**, 2911–2920 (2015). https://doi.org/10.1007/s12517-014-1304-3

Yilmaz, I., Kaynar, O.: Multiple regression, ANN (RBF, MLP), and ANFIS models for prediction of the swell potential of clayey soils. Expert. Syst. Appl. **38**(5), 5958–5966 (2011)

Authors and Affiliations

Frank I. Aneke[1] · Kennedy C. Onyelowe[2] · Ahmed M. Ebid[3]

[1]   Geotechnics and Materials Development Research Group (GMDRg) Civil Engineering
      Department, University of KwaZulu-Natal, Durban 4004, South Africa

[2]   Department of Civil and Mechanical Engineering, Kampala International University, Kampala,
      Uganda

[3]   Department of Structural Engineering, Faculty of Engineering and Technology, Future
      University, New Cairo, Egypt